Chinese Chemical Letters 34 (2023) 107454

Contents lists available at ScienceDirect

Chinese Chemical Letters

journal homepage: www.elsevier.com/locate/cclet

A three-dimensional polycyclic aromatic hydrocarbon based covalent organic framework doped with iodine for electrical conduction

Ruofan Li[a], Guolong Xing[b,*], Hui Li[c], Shen Li[a,*], Long Chen[a,*]

[a] Department of Chemistry, Tianjin Key Laboratory of Molecular Optoelectronic Science, Tianjin University, Tianjin 300072, China
[b] Zhejiang Engineering Laboratory for Green Syntheses and Applications of Fluorine-Containing Specialty Chemicals, Institute of Advanced Fluorine-Containing Materials, Zhejiang Normal University, Jinhua 321004, China
[c] State Key Laboratory of Inorganic Synthesis and Preparative Chemistry, Jilin University, Changchun 130012, China

ARTICLE INFO

Article history:
Received 1 April 2022
Revised 14 April 2022
Accepted 20 April 2022
Available online 25 April 2022

Keywords:
Three-dimensional
Covalent organic frameworks
Imine linkage
Chemical doping
Electrical conduction

ABSTRACT

Covalent organic frameworks (COFs) are a class of crystalline porous organic materials with variable structures and fascinating properties. The intrinsic low conductivity impedes their widely application in optoelectronic. Iodine doping is an effective way to enhance the electrical conductivity of COFs. Here, a novel 3D imine COF with *lvt* topology is synthesized from two different pentacene derivatives with the same core in the form of structural complementarity. DDHP-COF is a highly crystalline material featuring high surface area of 1679 m^2/g and excellent thermal stability up to 490 °C. Upon doping with iodine, the electrical conductivity can reach as high as 1.5×10^{-2} S/m which is significantly enhanced over 6 orders of magnitude compared with the pristine COF.

Covalent organic frameworks (COFs) are an emerging class of crystalline porous organic materials with extended structures entirely composed of organic linkers and connected by specific linkages [1]. With the advent of first 2D boronate ester COFs in 2005 [2], large amounts of COFs bearing different linkages, geometries and dimensionalities have been developed by different synthetic strategies following the principles of reticular chemistry [3–7]. Thanks to the fascinating structural tuneability, low density and exceptional high surface area, COFs have demonstrated great application potentials in many promising fields, such as gas adsorption and separation [8,9], sensing [10,11] and catalysis [12,13]. However, the intrinsic conductivity of most reported COFs is still low, which greatly hinders their application in optoelectronics.

Chemical doping is an effective manner to enhance the electrical conductivity by forming charge transfer complexes [14]. Notably, iodine is a suitable dopant for chemical doping to improve the electrical conductivity of COF powder or thin film [15–20]. Very recently, our group synthesized two non-planar 2D COFs with a rhombus and a kagome lattice by using two different non-planar polycyclic aromatic hydrocarbons (PAHs), in which the electrical conductivity of *c*-HBC-COF can be significantly enhanced at least five orders of magnitude after doping with iodine [21].

Pentacene and its derivatives, as one of the state-of-the-art organic semiconductors, have been widely investigated in organic field effect transistors due to their high carrier mobility, high on/off ratio and low threshold voltage [22,23]. Iodine is also used as an effective electron acceptor to dope pentacene to increase the electrical conductivity [24–26]. Masaru *et al.* first demonstrated the iodine doping of pentacene thin film, and the value of electrical conductivity of doped film reached as high as 110 S/cm which was 11 orders of magnitude larger than that of as-deposited film [24].

Herein, a new 3D imine COF (DDHP-COF) was synthesized by Schiff base condensation *via* a solvothermal method using pentacene derivatives with formyl (DHP-CHO) and amino (DHP-NH_2) functional groups as the building blocks. The obtained DDHP-COF shows high crystallinity, large surface area and excellent thermal stability. The electrical conductivity of DDHP-COF was significantly enhanced after doping with iodine due to the formation of charge transfer complex, which provides a useful insight in the preparation of imine COFs with high electrical conductivity.

The imine-linked COF (DDHP-COF) was synthesized *via* the copolymerization of DHP-CHO with DHP-NH_2 in a mixture of mesitylene/1,4-dioxane (6:4, v/v) in the presence of 6 mol/L acetic acid aqueous at 120 °C for 72 h (Fig. 1a), and obtained as yellow powder in a 70% isolated yield. The chemical structure of DDHP-

* Corresponding authors.
E-mail addresses: xinggl@zjnu.edu.cn (G. Xing), shenli@tju.edu.cn (S. Li), long.chen@tju.edu.cn (L. Chen).

https://doi.org/10.1016/j.cclet.2022.04.052
1001-8417/

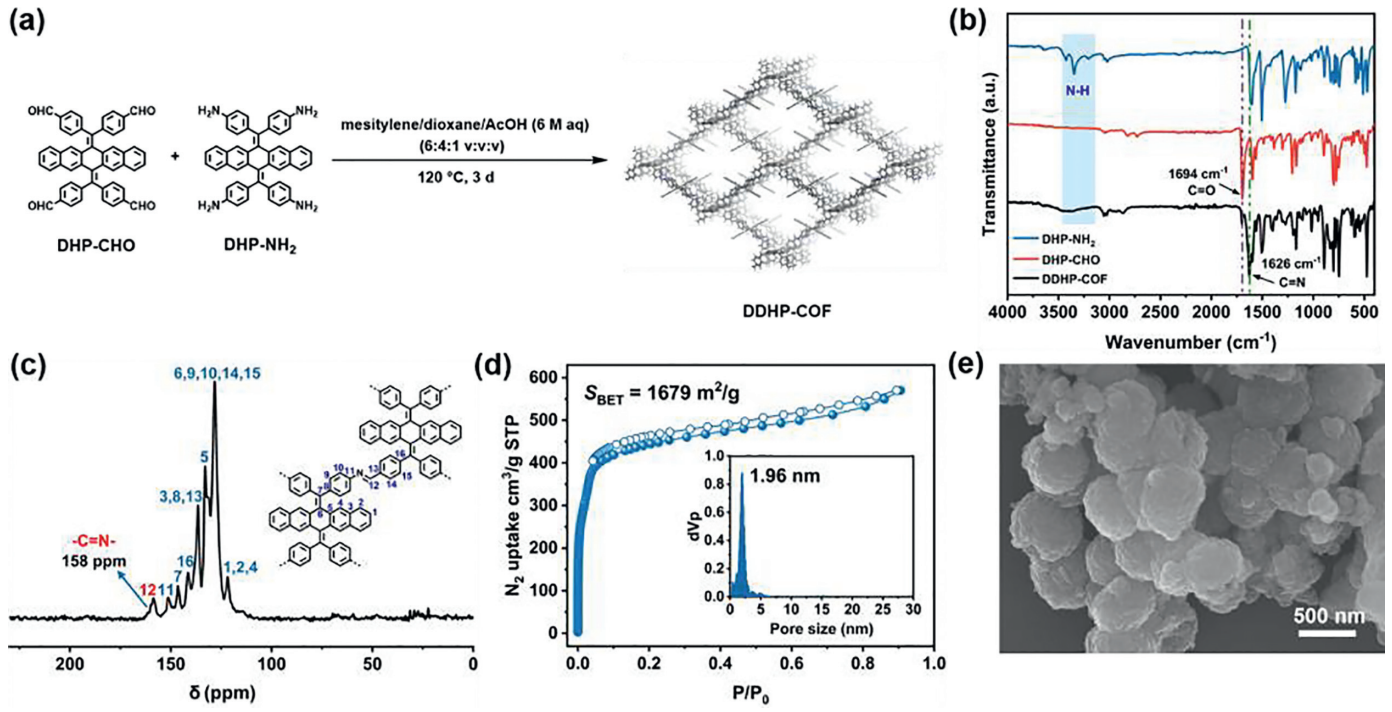

Fig. 1. (a) Schematic representation for the synthesis of DDHP-COF. (b) FT-IR spectra of DDHP-COF (black), DHP-CHO (red) and DHP-NH_2 (blue). (c) Solid-state ^{13}C NMR spectrum of DDHP-COF. (d) N_2 sorption isotherm of DDHP-COF. (e) SEM image of DDHP-COF.

COF was unambiguously characterized by a variety of different analytical techniques. As shown in Fourier transform infrared (FT-IR) spectra, the strongly attenuation of C=O stretching vibration (1694 cm^{-1} for DHP-CHO) and N−H vibration (3351 cm^{-1} for DHP-NH_2), as well as the appearance of typical stretching vibration band of C=N bond (1626 cm^{-1} for DDHP-COF), confirmed the successful condensation of aldehyde and amine groups and the formation of C=N bonds (Fig. 1b). Meanwhile, the characteristic peak at 158 ppm in the solid-state ^{13}C cross-polarization magic-angle-spinning (CP/MAS) NMR spectrum can be attributed to the carbon atoms in the newly formed imine linkages, again confirming the presence of C=N bonds (Fig. 1c). DDHP-COF showcased a uniform sphere-shaped morphology (Fig. 1e), as revealed by scanning electron microscopy (SEM) and transmission electron microscopy (TEM, Fig. S4 in Supporting information).

The permanent porosity of DDHP-COF was evaluated by N_2 sorption measurement at 77 K. The N_2 adsorption-desorption isotherms of DDHP-COF show a sharp adsorption at low pressure, which reveals a typical characteristic of the microporous materials (Fig. 1d). The Brunauer-Emmett-Teller (BET) surface area and total pore volume of DDHP-COF are estimated to be 1679 m^2/g (Fig. S6 in Supporting information) and 0.88 cm^3/g ($P/P_0 = 0.99$), respectively. Furthermore, based on non-local density functional theory (NLDFT) method, the dominant pore size of DDHP-COF is centered at 1.96 nm, which is consist with the theoretical model (1.94 nm, Fig. S10 in Supporting information).

The crystallinity of DDHP-COF was examined by powder X-ray diffraction (PXRD) measurement, and the structure of DDHP-COF was further resolved by PXRD pattern in conjunction with the structural simulation. The PXRD of DDHP-COF reveals obvious diffraction peaks at 4.0°, 8.1°, 11.7°, 12.2°, 14.3°, 15.6° and 17.6°, corresponding to its (011), (022), (332), (242), (620), (404) and (154) facet, respectively (Fig. 2a). The full width half maximum (FWHM) for the (011) peak is 0.56°, and the corresponding crystallite size is calculated to be 15.0 nm according to the Scherrer equation, indicating good crystallinity of DDHP-COF. After building

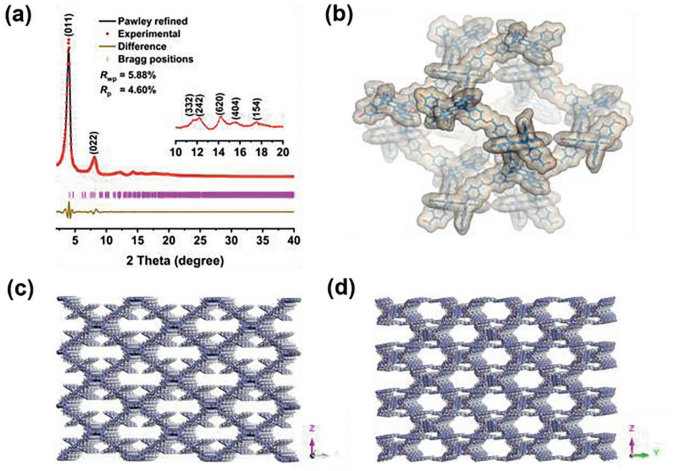

Fig. 2. (a) Experimental and refined PXRD patterns of DDHP-COF. (b) Structure representation of non-interpenetrated DDHP-COF. Structural representations of DDHP-COF viewed from (c) the *y* axis and (d) the *x* axis.

and optimizing the structural model by Materials Studio software package, DDHP-COF can be assigned to *IMMA* space group, and the optimized unit cell parameters were obtained as $a = 39.1815$ Å, $b = 38.3688$ Å, $c = 27.0927$ Å, $\alpha = \beta = \gamma = 90^o$. The PXRD pattern calculated from the simulated structural model agrees well with the experimental data, indicating DDHP-COF adopts the non-interpenetrated *lvt* topology (Figs. 2b-d). Full profile pattern matching (Pawley) refinement was applied to refine the experimental PXRD pattern, and provided a negligible difference between the experimental and Pawley refined patterns with good agreement factors ($R_p = 4.60\%$ and $R_{wp} = 5.88\%$).

The thermal stability of DDHP-COF was investigated by thermogravimetric analysis (TGA). As illustrated in Fig. S5 (Supporting information), DDHP-COF shows a high thermal stability up to 490

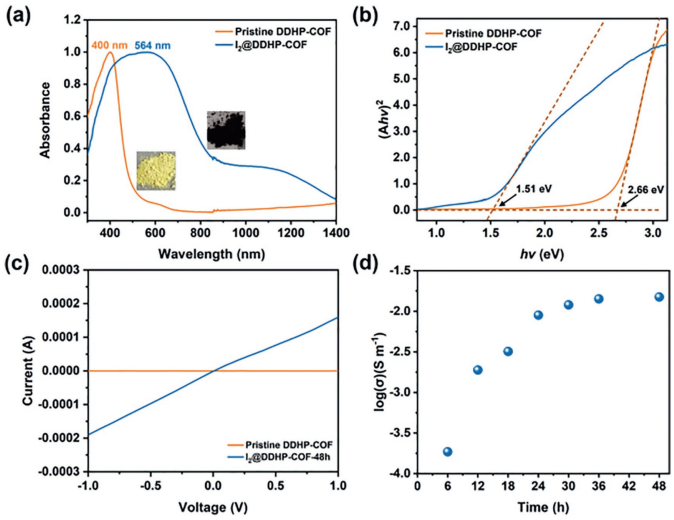

Fig. 3. (a) UV-vis-NIR spectra of pristine DDHP-COF (orange) and I_2@DDHP-COF (blue). (b) The band gaps of pristine DDHP-COF (orange) and I_2@DDHP-COF (blue) calculated by Tauc plot method. (c) *I-V* curves of pristine DDHP-COF and I_2@DDHP-COF-48 h. (d) Time-dependent electrical conductivity of DDHP-COF.

°C. Subsequently, DDHP-COF was immersed in different solvents, including tetrahydrofuran (THF), ethanol (EtOH), HCl (1 mol/L) and NaOH (1 mol/L) aqueous solutions, to evaluate the chemical stability of DDHP-COF (Scheme S3 in Supporting information). After immersing at room temperature for 3 days, DDHP-COF decomposes under HCl aqueous solution which can be attributed to the hydrolysis of imine bonds in the framework. Meanwhile, the weight loss is not obvious after immersing in the common organic solvents and NaOH aqueous solution (Table S1 in Supporting information), suggesting that DDHP-COF is stable under these conditions. Furthermore, negligible changes were observed in the FT-IR spectra (Fig. S7 in Supporting information), PXRD patterns (Fig. S8 in Supporting information) and N_2 sorption isotherms (Fig. S9 in Supporting information), indicating the framework structures, crystallinity and permanent porosity can be well-retained, which further confirms the chemical stability of DDHP-COF under the common organic solvents and basic conditions.

Iodine is commonly used for chemical doping to enhance electrical conductivity of COFs. In addition, COFs have been also reported as the iodine adsorbers as many other porous materials [27–30]. Inspired by this, the pristine DDHP-COF was doped by exposed to iodine vapour at 60 °C for a period of time and the iodine adsorption behaviour of DDHP-COF was investigated first. As shown in Fig. S12 (Supporting information), the capacity of iodine adsorption increases rapidly in the initial stage and gradually reaches adsorption equilibrium. After 48 h, the amount of iodine adsorption reaches maximum and the total adsorption capacity of DDHP-COF is 3.0 g/g (75 wt%), which is comparable to other porous materials [31–33]. Furthermore, with the increase of exposure time, the colour of DDHP-COF changes obviously from light yellow to black (Fig. 3a), indicating a varied optical band gap. Therefore, UV-vis-NIR absorption spectra of the pristine and iodine doped DDHP-COF (denote as I_2@DDHP-COF) were performed. Compared to the pristine DDHP-COF, the maximum absorption wavelength of iodine doped DDHP-COF exhibits a significant red shift and the broad absorption band extends to around 900 nm, which is consist with the colour change for DDHP-COF (Fig. 3a). The corresponding band gap calculated by Tauc plot method for DDHP-COF before and after I_2 doping also decreases from 2.66 eV to 1.51 eV (Fig. 3b), further confirming the change of optical band gap.

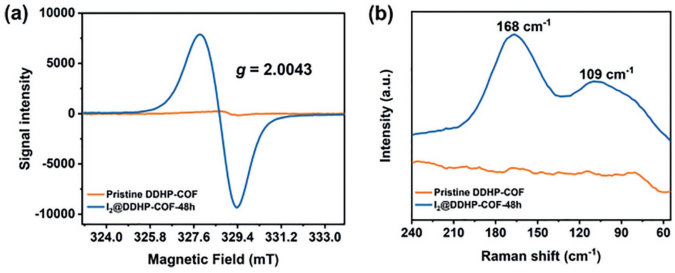

Fig. 4. (a) ESR spectra of pristine DDHP-COF (orange) and I_2@DDHP-COF–48 h (blue). (b) Raman spectra of pristine DDHP-COF (orange) and I_2@DDHP-COF–48 h (blue).

Subsequently, the current-voltage (*I-V*) measurement was performed to estimate the electrical conductivity of DDHP-COF with different I_2 doping time by a two-probe method. With the increase of iodine doping time, the current gradually increases and reaches maximum at 48 h (Figs. 3c and d). These results are summarized in Fig. S11 and Table S3 (Supporting information). Compared to pristine DDHP-COF, the electrical conductivity of I_2@DDHP-COF-48h is significantly enhanced and calculated to be 1.5×10^{-2} S/m, while the pristine DDHP-COF showed a negligible conductivity below 10^{-8} S/m, demonstrating that iodine doping can effectively enhance the electrical conductivity. As far as we know, this conductivity is comparable to the highest values of other iodine-doped COFs reported to date (Table S4 in Supporting information), such as JUC-518 (2.7×10^{-2} S/m) [19], 3D-sp^2-COF (2.79×10^{-4} S/m) [34], ZnPc-pz-I_2 (3.1×10^{-2} S/m) [35], FL-COF-1 (1.0×10^{-2} S/m) [36].

To investigate the origin for the electrical conductivity enhancement, electron spin resonance (ESR) measurement was performed. As shown in Fig. 4a, the pristine DDHP-COF displays a weak signal. In sharp contrast, an obvious paramagnetic signal centered at $g = 2.0043$ is observed for iodine doped DDHP-COF and the peak intensity significantly increases, indicating the formation of large amounts of organic radical species upon iodine doping that directly correlated with the electrical conductivity enhancement. In addition, the new absorption in the near infrared region of the UV-vis-NIR spectrum demonstrates the delocalization of free radicals and the generation of mixed-valence state between doped and undoped sites, which is also related to the electrical conductivity enhancement [20]. As further verified by the Raman spectra (Fig. 4b), the peaks appearing at 109 and 168 cm^{-1} for iodine doped DDHP-COF indicates the presence of I_5^- ions, suggesting the formation of charge transfer complex [37,38]. The stretching vibration in the FT-IR spectra of C=C bonds in the dihydropentacene motifs of DDHP-COF (1599 cm^{-1}) showcases a significant shift compared with iodine doped DDHP-COF (1579 cm^{-1}) which further confirms the charge transfer between I_2 molecules and DDHP-COF (Fig. S14 in Supporting information) [39]. To verify whether the DHP units in the framework are partially converted to the cyclodehydrogenated *c*-HBC units during the iodine doping, DHP-CHO was doped by iodine under the same conditions. After removing I_2, the residue was analyzed by ^1H NMR. As shown in Fig. S13 (Supporting information), the ^1H NMR spectrum exhibits no change compared with that of pristine DHP-CHO, demonstrating DHP units are stable during the iodine doping, therefore the formation of charge transfer complex is the main reason for the improvement of electrical conductivity.

The structural integrity of DDHP-COF after I_2 doping was investigated by PXRD and FT-IR measurements. After doping with I_2, the crystallinity of DDHP-COF disappeared. Interestingly, when the I_2 molecules were removed, the PXRD pattern could be recovered but the intensity decreased (Fig. S15 in Supporting information). Furthermore, the stretching vibration intensity of C=N bonds in the

FT-IR spectra still maintained with slight decrement after the removal of I_2, indicating that the framework of DDHP-COF was still retained.

In summary, we succeed to obtain a new 3D COF with non-interpenetrated *lvt* topology by the incorporation of the pentacene motif into the framework. The obtained DDHP-COF exhibits a high surface area and excellent thermal stability. Upon iodine doping, charge transfer occurs between iodine molecules and DDHP-COF to form positively charged radicals and negatively charged iodide counter anions. With the doping time prolonged, the charge carrier concentration increases, thus leading to the significant enhancement of the electrical conductivity compared with the pristine DDHP-COF. This work provides an effective method to improve the conductivity of COFs, and also provides a new opportunity for the application of doped COFs in the field of optoelectronics.

Declaration of competing interest

The authors declare that they have no known competing financial interests or personal relationships that could have appeared to influence the work reported in this paper.

Acknowledgment

This work was financially supported by the National Natural Science Foundation of China (Nos. 51973153, 22001191).

Supplementary materials

Supplementary material associated with this article can be found, in the online version, at doi:10.1016/j.cclet.2022.04.052.

References

[1] C.S. Diercks, O.M. Yaghi, Science 355 (2017) eaal1585.
[2] A.P. Côté, A.I. Benin, N.W. Ockwig, et al., Science 310 (2005) 1166–1170.
[3] D. Jiang, Chem 6 (2020) 2461–2483.
[4] S.Y. Ding, W. Wang, Chem. Soc. Rev. 42 (2013) 548–568.
[5] Y. Li, W. Chen, G. Xing, D. Jiang, L. Chen, Chem. Soc. Rev. 49 (2020) 2852–2868.
[6] M. Li, J. Liu, Y. Li, et al., CCS Chem. 2 (2020) 696–706.
[7] Y. Lv, Y. Li, G. Zhang, et al., CCS Chem. 3 (2021) 1773–1779.
[8] H. Furukawa, O.M. Yaghi, J. Am. Chem. Soc. 131 (2009) 8875–8883.
[9] H. Fan, A. Mundstock, A. Feldhoff, et al., J. Am. Chem. Soc. 140 (2018) 10094–10098.
[10] S.Y. Ding, M. Dong, Y.W. Wang, et al., J. Am. Chem. Soc. 138 (2016) 3031–3037.
[11] Z. Meng, R.M. Stolz, K.A. Mirica, J. Am. Chem. Soc. 141 (2019) 11929–11937.
[12] S.Y. Ding, J. Gao, Q. Wang, et al., J. Am. Chem. Soc. 133 (2011) 19816–19822.
[13] X. Wang, X. Han, J. Zhang, et al., J. Am. Chem. Soc. 138 (2016) 12332–12335.
[14] D.A. Stanfield, Y. Wu, S.H. Tolbert, B.J. Schwartz, Chem. Mater. 33 (2021) 2343–2356.
[15] S. Jin, T. Sakurai, T. Kowalczyk, et al., Chem. Eur. J. 20 (2014) 14608–14613.
[16] H. Ding, Y. Li, H. Hu, et al., Chem. Eur. J. 20 (2014) 14614–14618.
[17] S.L. Cai, Y.B. Zhang, A.B. Pun, et al., Chem. Sci. 5 (2014) 4693–4700.
[18] E. Jin, M. Asada, Q. Xu, et al., Science 357 (2017) 673–676.
[19] H. Li, J. Chang, S. Li, et al., J. Am. Chem. Soc. 141 (2019) 13324–13329.
[20] J.M. Rotter, R. Guntermann, M. Auth, et al., Chem. Sci. 11 (2020) 12843–12853.
[21] G. Xing, W. Zheng, L. Gao, et al., J. Am. Chem. Soc. 144 (2022) 5042–5050.
[22] M. Watanabe, K. Chen, Y.J. Chang, T.J. Chow, Acc. Chem. Res. 46 (2013) 1606–1615.
[23] R. Bhatia, D. Wadhawa, G. Gurtu, J. Gau, D. Gupta, J. Saudi Chem. Soc. 23 (2019) 925–937.
[24] T. Minakata, I. Nagoya, M.J. Ozaki, Appl. Phys. 69 (1991) 7354–7356.
[25] T. Minakata, I. Nagoya, M.J. Ozaki, Appl. Phys. 72 (1992) 4178–4182.
[26] R. Abdur, K. Jeong, M.J. Lee, J. Lee, Organ. Electron. 14 (2013) 1142–1148.
[27] X. Guo, Y. Li, M. Zhang, et al., Angew. Chem. Int. Ed. 59 (2020) 22697–22705.
[28] J. Chang, H. Li, J. Zhao, et al., Chem. Sci. 12 (2021) 8452–8457.
[29] Y. Xie, T. Pan, Q. Lei, et al., Angew. Chem. Int. Ed. 60 (2021) 22432–22440.
[30] P. Wang, Q. Xu, Z. Li, et al., Adv. Mater. 30 (2018) 1–7.
[31] Z. Yan, Y. Yuan, Y. Tian, D. Zhang, G. Zhu, Angew. Chem. Int. Ed. 54 (2015) 12733–12737.
[32] M. Golecki, N. Beyer, G. Steinfeld, et al., Angew. Chem. Int. Ed. 53 (2014) 9949–9952.
[33] D. Luo, Y. He, J. Tian, J.L. Sessler, X. Chi, J. Am. Chem. Soc. 144 (2022) 113–117.
[34] S. Wang, X.X. Li, L. Da, et al., J. Am. Chem. Soc. 143 (2021) 15562–15566.
[35] M. Wang, M. Wang, H.H. Lin, et al., J. Am. Chem. Soc. 142 (2020) 21622–21627.
[36] L. Wang, B. Dong, R. Ge, F. Jiang, J. Xu, ACS Appl. Mater. Interfaces 9 (2017) 7108–7114.
[37] M. Cazayous, A. Sacuto, Phys. Rev. B 70 (2004) 081309.
[38] C. Pei, T. Ben, S. Xu, S. Qiu, J. Mater. Chem. A 2 (2014) 7179–7187.
[39] A. Marinoiu, M. Raceanu, E. Carcadea, M. Varlam, Appl. Surf. Sci. 456 (2018) 238–245.